

A HYBRID NAVIER-STOKES / VISCOUS VORTEX PARTICLE WAKE METHODOLOGY FOR MODELING MANEUVER LOADS

L. S. Battey, L. N. Sankar
School of Aerospace Engineering
Georgia Tech, Atlanta, GA 30332-0150

Abstract

Maneuvering flight and high-speed flight are critical design points in any rotorcraft's operating envelope. These conditions give complex flow phenomena, creating high stresses and vibrations. To accurately predict the flow properties over the relatively flexible rotor blades, coupling between computational fluid dynamics (CFD) and computational structural dynamics (CSD) is required. In this work, GT-Hybrid, a hybrid wake rotorcraft CFD code that is coupled to DYMORE, is used. A vortex particle method has been implemented, in place of the existing lattice wake methodology. Selected UH-60A maneuvering flight conditions; being two diving-turn and pull-up maneuvers, are simulated using the vortex particle method. Results are compared qualitative with those using the traditional wake method and available experimental data; indicating that using the vortex particle method gives similar or better results. Additionally, computational efficiency is improved by using the vortex particle method and time savings exist in every simulation.

1. INTRODUCTION

1.1. Motivation

Rotary wing aircraft experience some of the most unique and complicated physical phenomena known to the aerospace community. At higher advance ratios, the inherently unsteady three-dimensional flow field produces compressibility effects on the advancing blade and dynamic stall on the retreating blade. The rotor blades also experience varying degrees of blade vortex interactions from neighboring blades. In maneuvering flight, aeroelastic effects are exacerbated and high stresses are endured by crucial structural components of the rotor and hub, governing the durability that must be achieved by the design. To operate in these maneuvers, along with forward flight, hovering, etc., the final design must come to fruition considering the influence of the many potential physical phenomena.

The accurate prediction of the aerodynamic effects and resulting loads on a rotorcraft's blades remains a paramount task in the aerospace industry. Experimental testing or high-fidelity analysis are often prohibitively expensive, making preliminary analysis tools a required part of the design process. Physics-based models are often desired due to their ability to study the effects of changing the specifics of the rotor design or flight condition. How effective these models are greatly depends on their accuracy and ease of use. Tools like this can greatly enhance the engineer's understanding of certain design requirements early in the process, saving time and cost.

1.2. State of the Art

With the cost of computing decreasing rapidly over the past few decades, the existing state of the art

rotorcraft codes has improved dramatically. Perhaps the most evident example of utilizing high computational power is using fine meshes encapsulating an entire rotor and its wake, often done using tools like OVERFLOW [1,2]. Users can employ grids with hundreds of millions of points to capture nearly any potential flow physics. Thus, with the use of high-end supercomputers, the current state of the art rotorcraft codes can determine the blades' aerodynamic loads so accurately that only a 0.2% error in the figure of merit is obtained [3]. This of course doesn't leave much room for improvement in terms of accuracy alone.

1.3. What is Missing

To obtain the most accurate possible solution from the current state of the art code could take weeks of runtime on a supercomputer with thousands of processors. Unfortunately, many researchers and designers wouldn't have this magnitude of computational resources readily available to them, and instead use lower fidelity tools for considerable time savings. The methodology used here, GT-Hybrid, which was introduced by Sankar et al. [4] and improved upon through many iterations [5,6], fits into this description. While this has shown to efficiently provide useful results, there is still thought to be room for improvement in both fidelity and computational time. Thus, it is desirable to implement a vortex particle wake methodology into GT-Hybrid, in place of the existing lattice methodology, to explore its potential benefits to accuracy or computational time. Inadequate research for the comparison of wake methods has been done thus far. Furthermore, the efficacy of using this alternative wake method to model unsteady maneuvering flight has yet to be determined. The purpose of this work is to help fill

the voids that previous research has left by exploring potential differences between two Lagrangian wake methods that can be used in a hybrid wake rotorcraft CFD code, such as in the computational time, resulting accuracy, or other unique qualities.

2. NUMERICAL FORMULATION

2.1. CFD Methodology

GT-Hybrid employs a hybrid wake methodology, meaning that the flowfield is only resolved within a small gridded domain surrounding a single rotor blade. Within this grid, the discretized Navier-Stokes solutions are found using a time-accurate flux-limited MUSCL scheme with 3rd order spatial and 1st order temporal accuracy. The turbulence model used here is the Spalart-Allmaras Detached Eddy Simulation (SA-DES) model [7]. The selecting of these specific parameters for solving the gridded domain have been shown to be an ideal balance of accuracy and computational time required [8]. Outside of this small gridded domain, the wakes of other blades are efficiently modelled with a grid-free field of vorticity elements, explained more later.

2.1.1 Computational Grid

GT-Hybrid uses a C-H grid topology, which has a single block that wraps around the airfoil surface. This type of grid has a well-defined, simple structure to it which allows for fast grid generation with automated programs. The grid used in this work for the UH-60A is shown below in Figure 1:

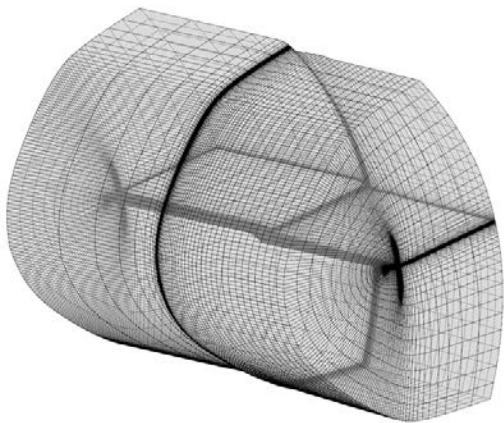


Figure 1 – C-H Grid for UH-60A Blade

This grid has dimensions of 131x65x45, corresponding to the chordwise, spanwise and normal directions, respectively. A resolution study has been done for this domain using 131x65x45, 263x65x90, and 263x128x90 sized grids. The coarsest grid used here was shown to be optimal in terms of accuracy and computational time [9].

Throughout the azimuthal range, pitching, flapping, and lead-lag motions are prescribed by an input file. This file can be manually entered by the user for a rigid blade simulation or created through CSD/CFD coupling with comprehensive rotorcraft code. For non-rigid blades, the blade-motions file includes structural deformations due to elasticity, which are enforced by deforming the grid within GT-Hybrid.

2.1.2 Lattice Wake Model

The wake model in GT-Hybrid represents the rotor blades with lifting lines, where vorticity elements are generated at several radial stations. From the quarter chord lines, the wake geometry and vorticity strengths are initialized as a perfectly helical structure using an analytical model [10]. The lattice wake model, traditionally used in GT-Hybrid, consists of a lattice of tip-to-tail Biot-Savart vectors being in the azimuthal direction for trailing vortices and the spanwise for shed vortices. A visualization of the lattice wake model for a single blade is shown in Figure 2:

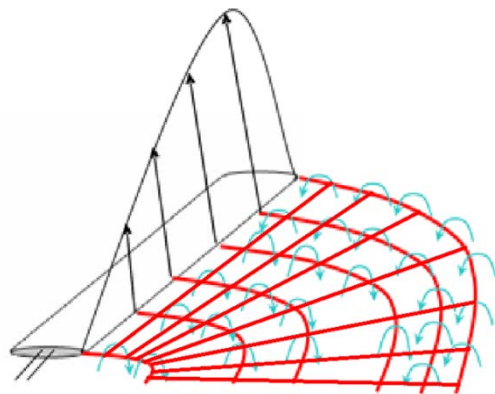


Figure 2 – Lattice Wake Method Visual

The strength of the vortices depends on the changes in bound circulation on the blade, which is calculated from the Navier-Stokes solution as the simulation progresses. A wake time step is set by specifying the azimuth interval to generate vortex filaments and delete the oldest ones. Also, at each wake time step, the wake convects from its own induced velocity, and the induced velocity on the grids boundaries is calculated. Since only one blade is gridded, but there are several blades, periodicity is enforced to generate their vortices. Vortex filaments inside the gridded region are not accounted for, as their effects are inherently captured in the Navier-Stokes solution. To determine the induced velocity from this lattice wake at any given point, the impact from each filament is found with the following formula:

(1)

$$\vec{V}_{ind} = \sum_{i=1}^N \left(\frac{\left(\frac{\Gamma}{4\pi} \vec{r}_1 \times \vec{r}_2 \right) |r_1 + r_2| \left(1 - \frac{\vec{r}_1 \cdot \vec{r}_2}{|r_1 r_2|} \right)}{|r_1 r_2|^2 - (\vec{r}_1 \cdot \vec{r}_2)^2 + r_c^2 (r_1^2 + r_2^2 - 2\vec{r}_1 \cdot \vec{r}_2)} \right)_i$$

where Γ is the vorticity strength and \vec{r}_1 and \vec{r}_2 are vectors from the point in question to the tip and tail of a Biot-Savart vector, respectively. r_c is a scalar called the core radius, with the implementation here representing the Vatisas core model [11]. A core radius growth model is used, introduced by Bhagwat and Leishman [12], which models weakening of vortices as they age.

2.2. CSD and Coupling

In accurately predicting the aerodynamics loads on a rotorcraft's blades, CFD alone is often not sufficient. One issue is that the collective and cyclic pitch inputs are often unknown. Also, the CFD alone provides no information about deformations due to blade elasticity, flapping, or lead-lag angles, motions that could significantly change the resulting aerodynamic loads. As such, these aspects need to be solved for externally.

2.2.1 CSD Methodology

The computational structural dynamics (CSD) methodology utilized here is DYMORE 2 [13]. This code employs geometrically exact finite element analysis to numerically solve for component deflections without making assumptions. Many components of the rotor can be modeled with a multibody dynamics approach. The UH-60A rotor modeled here features four fully articulated blades. Forces, moments, and deflections are then calculated on the many components as a function of azimuth for structural loading analysis and comparison with experimental data.

DYMORE 2 is also a rotorcraft comprehensive code, meaning it performs complete trimmed aeroelastic analysis with a stand-alone run. This is accomplished with a built-in lifting line aerodynamics solver that uses a 2-D lookup airfoil table and a non-linear inflow model. Also available and used in this work is an autopilot feature, where the user can set thrust and hub moment targets for the solver to aim for.

2.2.2 Coupling Methodology

While comprehensive codes and CSD are essential, their aerodynamic models are typically inferior to CFD, so the two codes can be used in conjunction. This is generally done by employing either a tight or loose coupling method. Tight coupling is performed by transferring information between the CFD and CSD codes at every time

step. The loose coupling approach transfers information periodically between solvers; here an entire rotor revolution at a time. Tight coupling is a more rigorous method, however, it complicates the numerical method and achieving trim can be difficult. With the codes used in this work, tight coupling has been shown to take about 2.5x the run-time as loose coupling but provides similar solutions [14]. As such, the loose coupling methodology is adopted for this work with a delta-trim formulation [15]. This method is shown schematically in Figure 3:

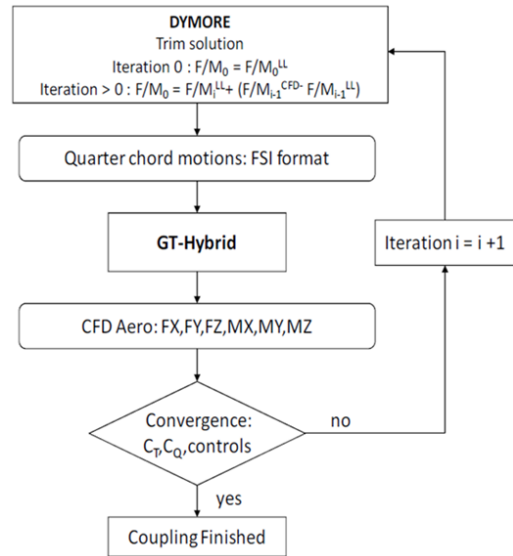


Figure 3 – Delta-Trim Loose Coupling Method

The aerodynamic loads are first calculated with only DYMORE largely to conduct the trim. The pitch controls are then fed into GT-Hybrid, which better approximates the airloads and used them to increment the airloads in a following DYMORE run, yielding new trim and elasticity results. Iterations are done until the thrust and hub moments converge.

2.3. Vortex Particle Methodology

The vortex particle method is an alternative approach to modelling vorticity that can also be applied to rotor wakes. Researchers have previously implemented vortex particle methods in different applications and achieved results that demonstrated its feasibility in rotorcraft aerodynamics [16]. It has even been observed that good agreements are seen with a lattice method [17], which has been traditionally used in GT-Hybrid. Explained here are some details of the vortex particle method and how it is implemented into GT-Hybrid in place of the traditionally used wake model.

2.3.1 Model Uniqueness

Many of the traits of the vortex lattice method are shared with the present implementation of the vortex particle method in GT-Hybrid. They both use the lifting lines to produce periodic vorticity elements that convect and impose velocity on the rotating C-H grid. Furthermore, they both begin with perfectly helical wakes that evolve as the solution progresses. The fundamental difference between the two models, however, is that instead of using vorticity trailers comprised of many tip-to-tail Biot-Savart vectors, the vortex particle method models the wake as many independent points, each with their own vector-valued vorticity. This takes away the stipulation of requiring each vortex vector to be connected. As the wake convects and the vortex elements convect and depart, enforcing the vortex vectors to stay in a lattice may be non-physical, meaning the particle method has potential accuracy benefits. The particle method also allows for the use of less computationally intensive equations to solve for each element's induced velocity, having potential to decrease the computational time. Additionally, trailing and shed wake components can both be accounted for by a vortex particle. These need separate filaments in the lattice method to keep the components tip-to-tail. This alone would make the vortex particle method twice as fast, with all other things equal. It also means it requires less memory, making it more scalable if desired.

2.3.2 Induced Velocity

Finding the vortex particle wake-induced velocity at any given point is done in an analogous manner to the Biot-Savart law, i.e. the two methods' vorticity vectors both follow the right-hand rule with respect to their induced velocities. The general function used to find the induced velocity caused by every particle at a certain point is as follows:

$$\vec{V}_{ind} = \sum_{i=1}^N K(|\vec{r}_i|) * (\vec{\alpha}_i \times \vec{r}_i) \quad (2)$$

where \vec{r}_i is a distance vector from the vortex particle to the point where the induced velocity is being determined and $\vec{\alpha}_i$ is a vorticity vector of a particle. $K(|\vec{r}_i|)$ is called the Biot-Savart kernel which is a scalar-valued function. The implementer of a vortex particle method has the freedom to choose a specific kernel to be used, and it generally depends on (at least) the distance from a vortex particle. Ultimately, the kernel is what controls the accuracy of the induced velocity calculation and can greatly contribute to the computation time required to solve for it. The Biot-Savart Kernel used in this work is as follows:

$$(3) \quad K(|\vec{r}_i| + r_{c,i}) = \frac{1}{4\pi(|\vec{r}_i| + r_{c,i})^3}$$

Here $|\vec{r}_i|$ is the magnitude of the distance vector from a vortex particle to the point where the induced velocity is to be calculated. The $r_{c,i}$ value is the core radius, which has the same growth model as in the lattice method. It is noticed that finding the induced velocity from the vortex particle method (equations 2 and 3) requires significantly less operations than for the lattice method (equation 1), indicating time savings.

2.3.3 Preliminary Validation

The details of the present implementation of the vortex particle method have been partially validated using some small-scale problems in a previous work [18] but are not shared in detail here for brevity. Studied was the impact of different Biot-Savart Kernels on the induced velocity calculation and how they compared with that from the lattice wake. The resolution of the vortex particle wake, i.e. how many particles to use, was also investigated. These studies indicated that the kernel in equation 3 was the optimal choice because of its superior computational time and comparable induced velocity values. Also, that the vortex particle wake can have the same number of elements as the lattice wake to give comparable results.

3. MANEUVER SIMULATIONS

Helicopters in maneuvering flight demonstrate some of the most complex and unique physical phenomena known to the rotorcraft community. Non-zero translational and angular accelerations experienced by the aircraft cause highly unsteady aerodynamic loads which can occur from operating beyond the airfoil's stall region. The flexible rotor blades can experience large elastic deformations, which intensify aeroelastic effects and cause excess vibratory loads in both the rotating and non-rotating components. The large vibratory load spectrum also is a cause for concern of catastrophic fatigue failure. Control loads in maneuvering flight have been observed to be even four times that experienced in high-speed forward flight [19]. As a result, loads during maneuvers typically are what govern the required strength and durability of crucial rotor and hub components. Incorrect prediction of the critical loads during an aircraft design program could lead under or oversized mechanical components, causing potentially serious issues in the future.

To analyze the efficacy of using vortex particle methodology in GT-Hybrid to model maneuvering

flight, individual revolutions of three extensively studied UH-60A flight tests are simulated. The maneuvers studied here all have various data on the blade aerodynamic loads, component structural loads, pilot input, etc. within the NASA-Army UH-60A Airloads Database [20]. First, two right-hand banking diving-turn maneuvers, test points 11679 and 11680, are simulated. Next a longitudinal pull-up maneuver, test point 11029.

Significant work has proceeded the author's which has led to validation of using GT-Hybrid and DYMORE loosely coupled to simulate the present maneuvering flight cases. Rajmohan [8] utilized and improved aspects of this approach while validating steady level flight simulations as well as the transient UTTAS 11029 pull-up maneuver [21], [22]. Marpu [9] simulated the diving turn maneuvers 11680 and 11679 [23], [24] and further refined and added to the knowledge of optimal modeling preferences. The present research effort represents the first instance of using a vortex particle methodology for studying maneuvering flight, meaning the newly conducted vortex particle simulations act as a controlled study with the lattice wake simulations acting as a baseline.

3.1. Diving Turn Maneuvers

Diving turn maneuvers exhibit a rotorcraft vertically descending as quickly as possible in high-speed forward flight while doing a banking turn. During a dive turn the rotorcraft utilizes its high potential and kinetic energy to maintain very high load factor. Within the flight tests, 11680 is ranked as being the most severe out of all the studied maneuvers, designated by the highest push-rod loads, torsion moment at 0.3R and chord bending moment at 0.113R.

The two dive turn maneuvers here are both characterized by a right-hand bank angle (θ_b), climb rate (V_z), average advance ratio (μ_{ave}) and an average normal load factor ($n_{z,ave}$). These values are outlined in Table 1 below:

Case	θ_b (deg)	V_z (ft/min)	μ_{ave}	$n_{z,ave}$
C11679	55	-3878	0.393	1.69
C11680	60	-5324	0.388	1.48

Table 1 – Dive Turn Case Parameter Averages

Each maneuver as recorded in the Airloads Catalog lasts about 9 seconds and 40 revolutions. The climb rate and banking angle are nominally constant in the most crucial part of the transient maneuver. The normal load factor is plotted against the advance ratio for each maneuver's duration in Figure 4 below:

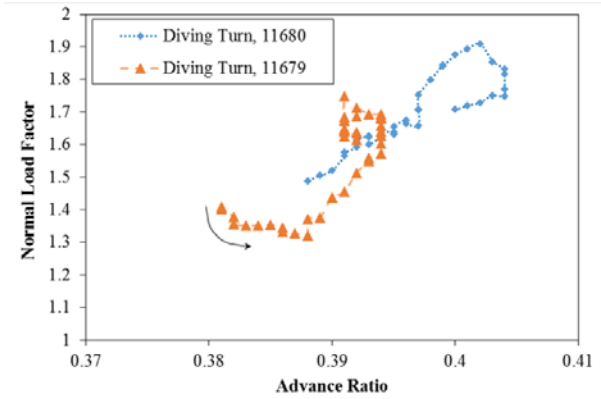


Figure 4 – Dive Turn Load Factor / Advance Ratio

The values plotted progress from the first revolution in the maneuver to the last in the direction of the arrows shown. Only the most severe revolutions of the maneuvers are studied here as they are considered the most important. For 11680, studied is revolution 12, and revolution 20 is studied in 11679, both of which are in the severe banking portion of the maneuver. At these revolutions for 11680 and 11679, the advance ratios are 0.401 and 0.394, with normal load factors of about 1.9 and 1.7, respectively.

3.1.1 Dive Turn 11680 Results

Various aerodynamic and structural loads for revolution 12 of dive turn 11680 can be seen in Appendix A. Only one radial station per load is selected for brevity, and the mean values are removed to avoid potential zeroing discrepancies in the experimental data.

First looking at the aerodynamic loads, a more outboard station of 0.865R was chosen to view. The results from using either wake look very similar, with the most differences occurring in the first quadrant. Overall, both wake methods capture the general wave form of the experimental data quite well, but some higher harmonics are lacking in the simulations. Two subsequent dynamic stall events are captured well near the last quadrant, most clearly indicated by the sudden drops in pitching moment. However, the magnitude of the negative lift on the advancing blade is underpredicted, along with the peak beforehand.

For the structural loads, a relatively inboard station of 0.5R was chosen to view. The structural response in the experimental data appears to have dampened out much of the extremely high frequency that was seen in some aerodynamic loads. For the torsional bending, both wake methods look near identical to each other. The flapwise bending shows that some high harmonics are being overpredicted by either wake method. The vortex particle results predict some of these

amplitudes as being lower, which helps the correlation here. Conversely, the vortex particle method underpredicts the medium frequencies in the chordwise bending more, hurting correlation. The peak to peak pitch link loads are the highest here compared to any other UH-60A condition, and this magnitude is captured quite well. However, the loading greater than 1-3 per rev greatly lacking in the simulations.

3.1.2 Dive Turn 11679 Results

Aerodynamic and structural loads for revolution 20 of 11679 are shown in Appendix B, having the same format and radial locations as before. The general trend of underpredicting higher harmonics remains in these simulations. Some high loads in the first quadrant are not sufficiently captured by either wake method. The amplitude of negative lift in the first quadrant is better predicted than in the last dive turn, and the vortex particle method predicts its phase slightly better here, and in general throughout all loads. The structural loads show that results from both wake methods give similar trends as before, with the vortex particle method predicting some phases and amplitudes better. The peak to peak pitch link loads are overpredicted by about 50% here by either wake method, with the loading waveform appearing better in the vortex particle result except in the last quadrant.

3.2. Pull-Up Maneuver

A pull-up maneuver is defined as when a rotorcraft tilts its nose upwards sharply in forward flight to climb as quickly as possible. The specific pull-up maneuver studied here is designated as flight test point 11029, which is based on a Utility Tactical Transport Aerial System (UTTAS) in the original UH-60A design specification [25]. Extensive data from this is again included in the UH-60 Airloads Catalog [20]. In the flight database, 11029 is ranked as the second most severe condition, with the highest flapwise bending moment at 0.113R and third highest oscillatory pitch link load. 11029 begins with level flight at a high advance ratio of $\mu = 0.360$ (much like the 8534 condition), but after a longitudinal pull-up then push-over the speed reduces to a final advance ratio of $\mu = 0.220$. This effectively draws upon the rotorcraft's high kinetic energy to increase the altitude.

Again, only the most severe revolution is studied, here being revolution 16. This represents about halfway into the pull-up where the speed is already reduced from 158 to 139 knots and a maximum load factor of 2.1 occurs. For several revolutions surrounding 16, the flight condition significantly exceeds the steady state McHugh lift boundary [26], where the thrust parameter peaks at $n_z C_W / \sigma$

$\sigma = 0.165$ compared to the upper stall limit of 0.12 [27]. The $n_z C_W / \sigma$ vs. μ throughout the entire 11029 maneuver are shown in comparison to the McHugh lift boundary along with other UH-60A test conditions in Figure 5:

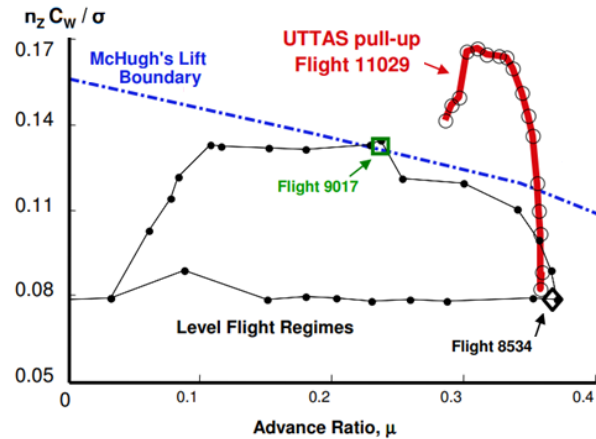


Figure 5 – Flight Tests vs. McHugh Boundary [26]

Because of this extreme condition, several stall events occur during this maneuver throughout the azimuthal range, including at outboard radial stations of the advancing blade. Furthermore, in this pull-up, the wake passes through the rotor disk before being blown downstream, making simulation with a hybrid wake a challenging task.

3.2.1 Pull-Up 11029 Results

Aerodynamic and structural loads for revolution 16 of 11029 are shown in Appendix C, having the same format and radial locations as before. Some of the trends observed in the aerodynamic loads of the dive turns are also observed for this pull-up, such as the lack of very high frequency effects. However, some harmonic content beyond 3P is being seen in the simulations more so than the dive turns. Here the two stall cycles on the retreating side are seen to be captured, evident in both the normal loads and pitching moments. The vortex particle method appears to be capturing these stall events better in both amplitude and phase. Stall on the advancing side is seen in the simulations, with the vortex lattice results showing it with a greater magnitude than the particle method here. However, the effects on the advancing side appear to be simulated significantly out of phase with respect to the experiment for both wake methods, so it's uncertain which is more accurate. Overall, the simulations appear to be doing better here at capturing the higher harmonics, peak-to-peak, and general waveform than for the dive turns.

For the torsional bending, the results from either wake method are quite close to each other, with the lattice results slightly leading in phase. The higher

harmonics of the torsional bending are not captured adequately in the first and second quadrants and are simulated out of phase for the last two quadrants, with the vortex particle method looking better here. Looking at the flapwise and chordwise bending, the vortex particle results appear to fit the experiment much better in the first and second quadrants, especially for the inboard radial stations. Above about 225 degrees azimuth, however, the simulations are significantly out of phase, with the vortex lattice solution typically predicting the amplitudes as being larger. The peak to peak pitch link loads are overpredicted, but not as much as for 11679, and more harmonic content is seen in the last two quadrants here, with no clear indication of which wake method is correlating better overall.

3.3. Computational Time

Because the numerical modeling parameters for each case was the same, the computational times were also the same. The simulations were conducted using a 12-processor desktop Linux machine, and some wall-clock times comparing wake methods are shown in Table 2:

Time For:	Lattice Wake	Particle Wake
Wake Iter.	9.77 secs	1.35 secs
CFD Sim.	85.37 mins	68.60 mins
CFD/CSD Iter.	2.38 hrs	1.95 hrs

Table 2 – Computational Times

The wake iteration time is defined as the total time associated with the wake that occurs every wake time step. It is seen that by using the vortex particle method, this time is reduced by about a factor of 8. The time for one standalone CFD simulation consists of two rotor revolutions. This time decreases by about 25%, of course less than the wake iteration since this time is only a part of the total CFD simulation. The time for one CFD/CSD coupling iteration includes that CFD time plus the time required for DYMORE 2. This time decreases by about 20% by using the vortex particle method in GT-Hybrid. The number of coupling iterations required for trim convergence is normally 8-10 but never more than 15.

4. CONCLUSIONS

In this work, the hybrid Navier-Stokes/free wake model CFD code, GT-Hybrid, was supplemented with the vortex particle wake in place of the existing lattice wake methodology. Simulations were conducted with both wake methods, using loose coupling with DYMORE 2, for the UH-60A rotor in three maneuvering flight conditions. Comparing the

results with the experimental data showed that the general waveform and peak to peak of the loading is generally captured well, but some higher harmonics are missing in the simulations. The results from the vortex particle wake were overall quite like the lattice method, occasionally showing a decrease in amplitudes of some higher harmonics. This appeared to help the correlation in some cases but hurt it in others. The computational time savings from using the vortex particle method were significant, decreasing by about 25% for a stand alone CFD simulation and by about 20% with CFD/CSD coupling. Because of this and potentially some accuracy benefits, the vortex particle method is seen as an improvement to GT-Hybrid overall. Ultimately, the present research expands the understanding of the vortex particle method and its behavior when applied to rotorcraft aerodynamics in maneuvering flight.

Acknowledgements

This research effort was sponsored by the US Government under Other Transaction Agreement number W15QKN-10-9-0003 between Vertical Lift Consortium, Inc. and the Government. The U.S. Government is authorized to reproduce and distribute reprints for Government purposes notwithstanding any copyright notation thereon. The views and conclusions contained in this document are those of the authors and should not be interpreted as representing the official policies, either expressed or implied, of the U.S. Government.

Copyright Statement

The authors confirm that they, and/or their company or organization, hold copyright on all of the original material included in this paper. The authors also confirm that they have obtained permission, from the copyright holder of any third party material included in this paper, to publish it as part of their paper. The authors confirm that they give permission, or have obtained permission from the copyright holder of this paper, for the publication and distribution of this paper as part of the ERF proceedings or as individual offprints from the proceedings and for inclusion in a freely accessible web-based repository.

References

- [1] Ahmad J., Duque, E. P. N., and Strawn, R. C., "Computations of Rotorcraft Aeroacoustics with a Navier-Stokes/Kirchhoff Method," 22nd European Rotorcraft Forum, Brighton, UK, Sept 1996.
- [2] Bauchau, O. A. and Ahmad, J. U., "Advanced CFD and CSD Methods for Multidisciplinary Applications in Rotorcraft Problems", Proceedings

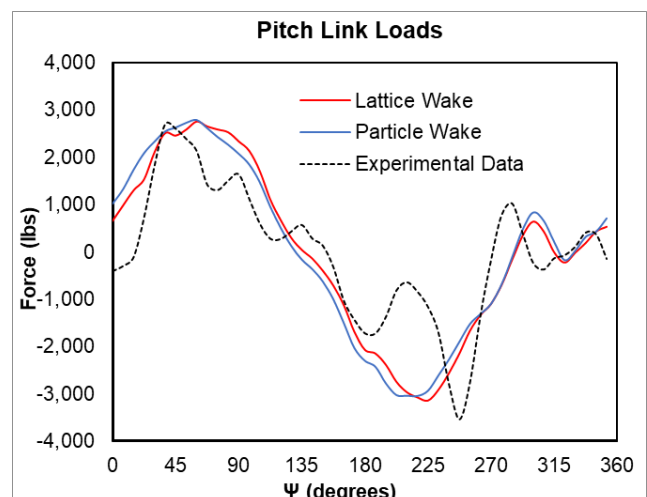
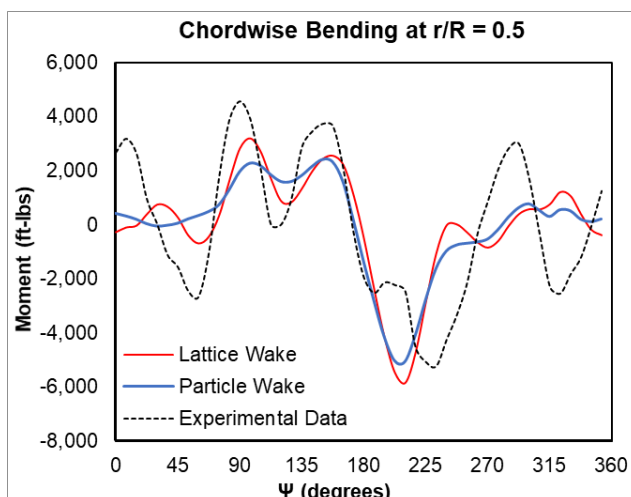
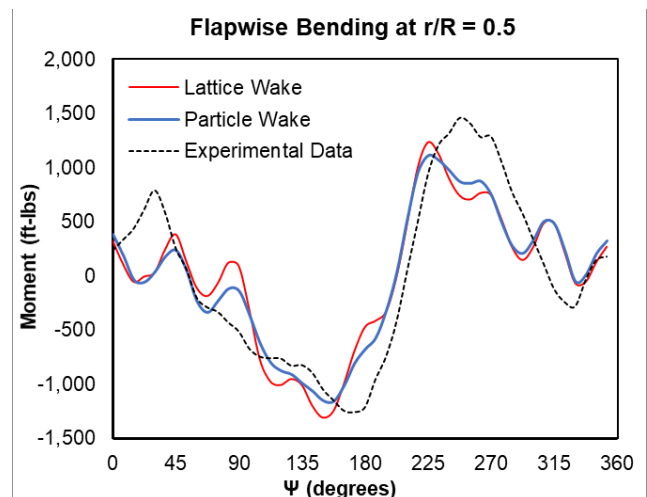
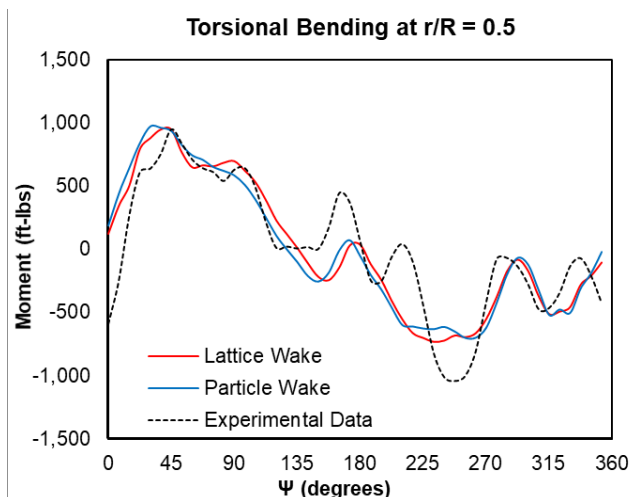
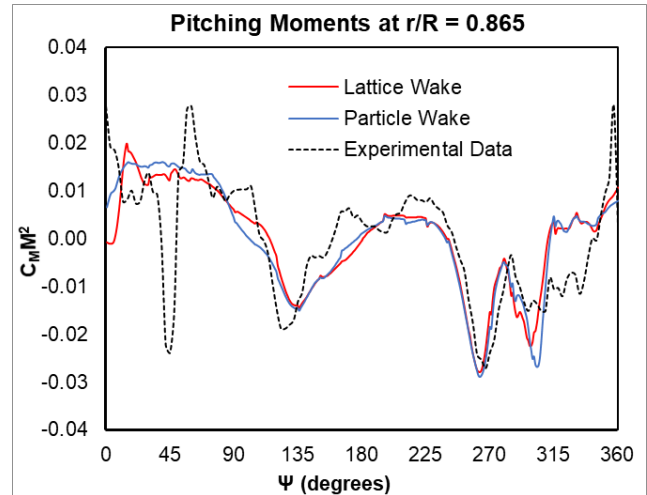
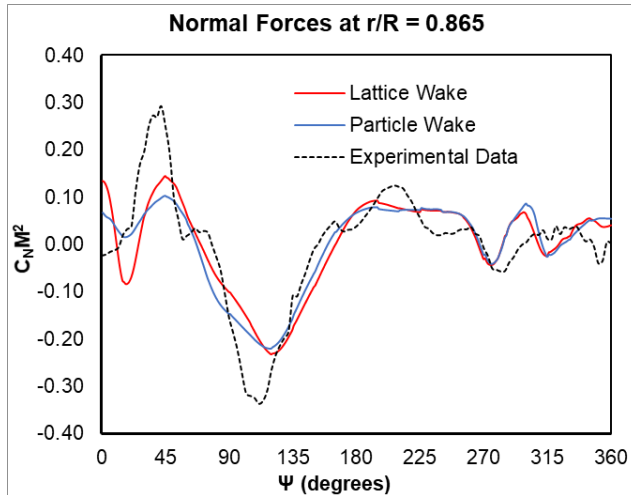
of the AIAA/NASA/USAF Multidisciplinary Analysis and Optimization Symposium, Bellevue, WA, Sep. 4-6, 1996, pp.945-953.

- [3] Chaderjian, N. and Ahmad, J. "Advancing Rotorcraft Simulation Using Computational Fluid Dynamics," *NASA Ames Research Center*, 2015. www.nas.nasa.gov/SC13/demos/demo4.html
- [4] Sankar, L. N., Bharadwaj, B. K., and Tsung, F. L., "A three-dimensional Navier-Stokes/full-potential coupled analysis for viscous transonic flow," AIAA 10th Computational Fluid Dynamics Conference, Honolulu, HI, June 24-27, 1991
- [5] Berezin, C. R. and Sankar, L. N., "An Improved Navier-Stokes/Full Potential Coupled Analysis for Rotors," *Mathematical Computational Modeling*, Vol.19, No.3/4, 1994, pp.125-133.
- [6] Yang, Z., Sankar, L. N., Smith, M. J., and Bauchau, O., "Recent Improvements to a Hybrid Method for Rotors in Forward Flight," *Journal of Aircraft*, Vol. 39, No. 5, 2002, pp. 804-812.
- [7] Spalart, P. R. and Allmaras, S. R., "A One-Equation Turbulence Model for Aerodynamic Flows," *La Recherche Aerospaciale*, 1994.
- [8] Rajmohan, N. "Application of Hybrid Methodology to Rotors in Steady and Maneuvering Flight," Dissertation: School of Aerospace Engineering. Georgia Institute of Technology, Atlanta, GA, 2010.
- [9] Marpu, R. "Physics Based Prediction of Aeromechanical Loads for UH-60A Rotor," Dissertation: School of Aerospace Engineering. Georgia Institute of Technology, Atlanta, GA, 2013.
- [10] Mello, O. A. F., Prasad, J. V. R., Sankar, L. N., and Tseng, W., "Analysis of Helicopter/Ship Aerodynamic Interactions", *American Helicopter Society Aerodynamics Specialists Conference*, San Francisco, California, Jan. 19-21, 1994.
- [11] Vatistas, H., Kozel, V., Mih, W. "A Simpler Model for Concentrated Vortices." *Experiments in Fluids* Vol. 11, No. 1, 1991, pp. 73-76.
- [12] Bhagwat, M., Leishman G. "Generalized Viscous Vortex Model for Application to Free-Vortex Wake and Acoustic Calculations," *Annual Forum Proceedings-American Helicopter Society*. Vol. 58, American Helicopter Society, Inc., 2002, pp. 2042-2057.
- [13] Bauchau, O. A. "Computational Schemes for Flexible, Nonlinear Multi-Body Systems," *Multibody System Dynamics* Vol. 2, No 2. 1998, pp. 169-225. DOI: 10.1016/S0895-7177(00)00303-4
- [14] Altmikus, A., Wagner, S., Beaumier, P., and Servera, G. "A comparison- Weak versus strong modular coupling for trimmed aeroelastic rotor simulations," *AHS International, 58th Annual Forum Proceedings*. Vol. 1, 2002, pp. 697-710.
- [15] Tung, C., Caradonna, F. X., and Johnson, W. R. "The prediction of transonic flows on an advancing rotor," *Journal of the American Helicopter Society* Vol. 31, No. 3, 1986, pp. 4 -9. dx.doi.org/10.4050/JAHS.31.4
- [16] He, C. and Zhao, J. "Modeling Rotor Wake Dynamics with Viscous Vortex Particle Method," *AIAA Journal* Vol. 47, No. 4, 2009, pp. 902-915.
- [17] Leonard, A. "Computing Three Dimensional Incompressible Flows with Vortex Elements," *Annual Review of Fluid Mechanics* Vol. 17, 1985, pp. 523-559.
- [18] Battey, L. "A Hybrid Navier-Stokes/Vortex Particle Wake Methodology for Modeling Helicopter Rotors in Forward Flight and Maneuvers," Dissertation: School of Aerospace Engineering. Georgia Institute of Technology, Atlanta, GA, 2018.
- [19] Kufeld, R, Bousman, W. "High Load Conditions Measured on a UH-60A in Maneuvering Flight," *Journal of the American Helicopter Society* Vol. 43, No. 3, 1998, pp. 202-211. <http://dx.doi.org/10.4050/JAHS.43.202>
- [20] Bousman, W. and Kufeld, R. "UH-60A Airloads Catalog," *Aeroflightdynamics Directorate (AMRDEC) U.S. Army Research, Development, and Engineering Command. Ames Research Center. Moffett Field, California, 2005. NASA/TM-2005-212827, AFDD/TR-05-003*
- [21] Rajmohan, N., Sankar, L., Costello, M. "Effect of Inflow Modeling on Coupling between Rotor Flight Mechanics and Aeromechanics," *49th AIAA Aerospace Sciences Meeting including the New Horizons Forum and Aerospace Exposition*. Orlando, FL, 2011.
- [22] Rajmohan, N., Marpu, R., Sankar, L. N., Baeder, J. D., and Egolf, T. A. "Improved prediction of rotor maneuvering loads using a hybrid methodology," *Annual Forum Proceedings-American Helicopter Society*. Vol. 67, 2011.
- [23] Marpu, R., Sankar, L. N., Makinen, S., Baeder, J. D., Egolf, T. A., and Wasikowski, M. "Physics based modeling of maneuver loads for rotor and hub design," *American Helicopter Society Specialist's Design Conference*. American Helicopter Society, Inc., San Fransisco, 2012.
- [24] Marpu, R., Sankar, L. N., Makinen, S., and Baeder, J. D. "Computational Modeling of Diving-Turn Maneuvers using Hybrid Methodology," *Annual Forum Proceedings American Helicopter Society*. Vol. 68, American Helicopter Society, Inc., Fort Worth, TX, 2012.
- [25] Abhishek, A., Ananthan, S., Baeder, J., and Chopra, I. "Prediction and Fundamental Understanding of Stall Loads in UH-60A Pull-Up Maneuver," *Journal of the American Helicopter Society*, Vol. 56, No. 4, 2011.
- [26] McHugh, F. J., "What Are the Lift and Propulsive Force Limits at High Speed for the Conventional Rotor?" *American Helicopter Society 34th Annual*

- [27] Bhagwat, M. J., Ormiston, R. A., Saberi, H. A. and Hong, X., "Application of CFD/CSD Coupling for

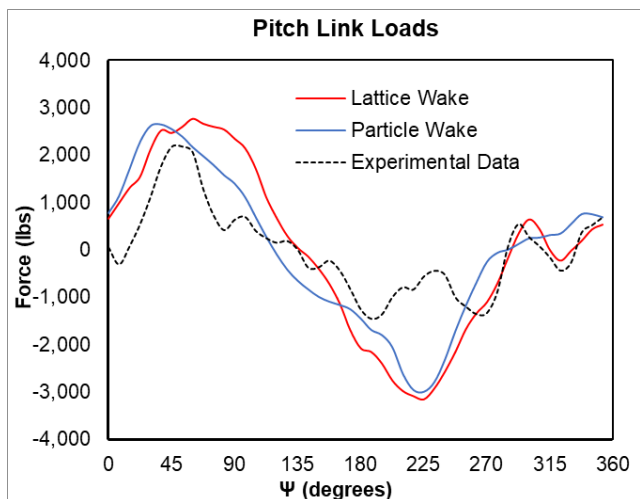
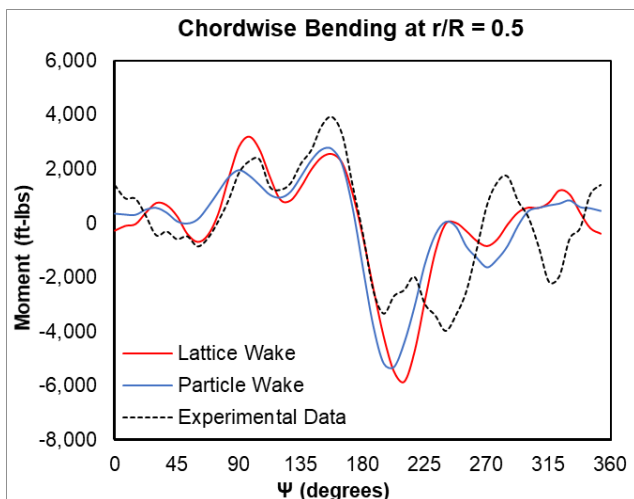
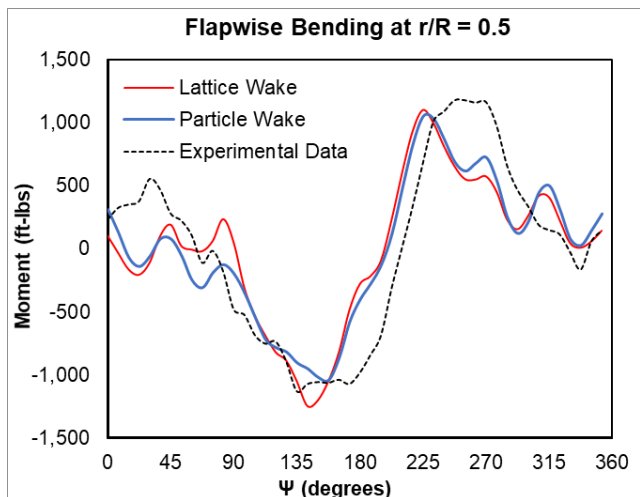
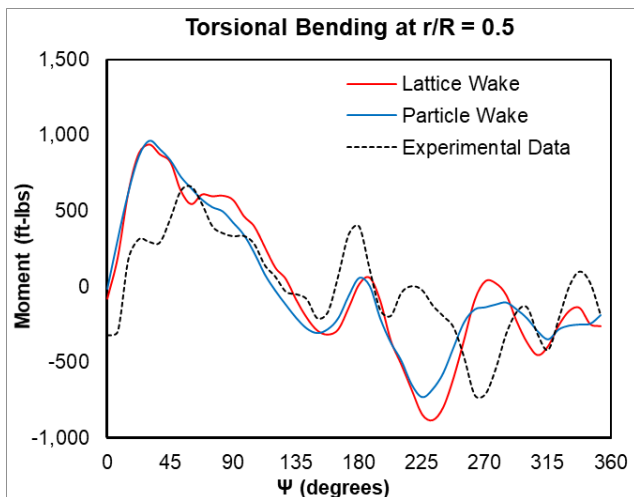
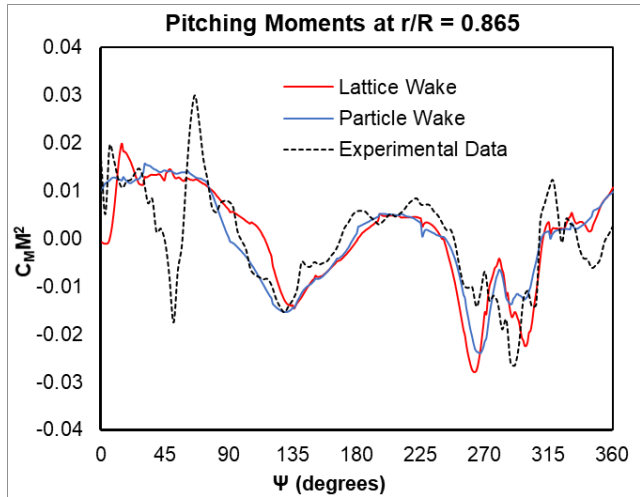
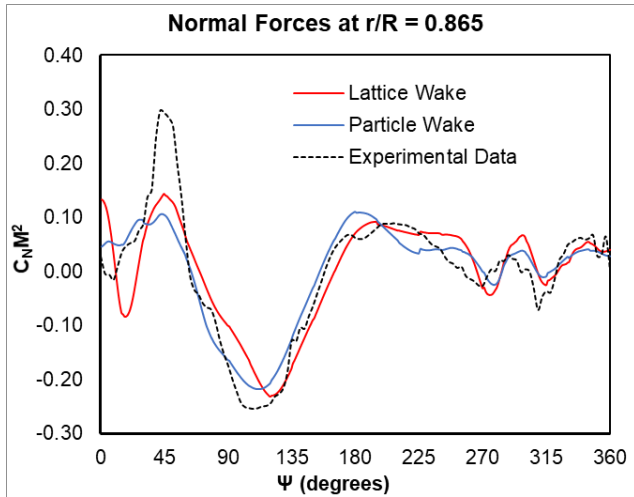
APPENDIX A:

UH-60A Dive-Turn Maneuver (11680, Revolution 12), Aerodynamic and Structural Loads



APPENDIX B:

UH-60A Dive-Turn Maneuver (11679, Revolution 20), Aerodynamic and Structural Loads



APPENDIX C:

UH-60A Pull-Up Maneuver (11029, Revolution 16), Aerodynamic and Structural Loads

